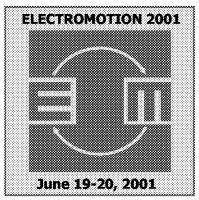

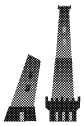

Bologna - ITALY

HIGH-FREQUENCY BEHAVIOR OF THREE-PHASE INDUCTION MOTOR WINDINGS

G. Grandi, U. Reggiani, C. Rossi, and G. Sancineto

Dept. of Electrical Engineering
University of Bologna
Italy

Abstract - The high-frequency behavior of induction motors is analyzed in this paper. Lumped equivalent circuits are proposed to account for the frequency-dependent phenomena in the motor stator winding and core. The proposed circuit models allow time- and frequency-domain analysis to be performed with standard circuit simulators in a wide range of frequency. Furthermore, common- and differential-mode conducted EMI can be predicted when the motor is supplied by switching converters.

I. INTRODUCTION

Nowadays, AC motor drives are widely used in electromechanical energy conversion systems. In the latest switching power converters the commutation times are very small and, as a consequence, the motor winding is subjected to a very large amount of HF voltage components [1], [2]. Owing to winding parasitic capacitances [3] (i.e., turn-to-turn and turn-to-iron capacitances), these HF voltage components cause HF leakage currents [4] and conducted Electromagnetic Interferences (EMI) in the power mains and ground system [5]-[7]. The resulting HF currents are classified in common- and differential-mode (CM and DM) components according to their circulation paths. The frequency range of interest for conducted EMI in power electronics is usually from tens of kHz up to tens of MHz [8]. Because of the high switching speed of MOSFETs and IGBTs, the nonideal behavior of the power converter elements plays an important role in the HF current component prediction. Thus, in order to model the HF behavior of the converter, it is necessary to take account of parasitic parameters in semiconductor devices and passive elements of the power circuit [9].

In the low to medium power range, the low voltage induction motor is the most frequently used type of motor. In this case, the stator winding is realized by a series connection of mush wound coils. Because of the random distribution of the turns for each coil, an analytical evaluation of the coil model parameters cannot be based on single-turn models such as in form wound coils [10], [11]. Hence, the lumped equivalent circuit of a single coil can be defined in terms of equivalent impedance by means of a suitable three-terminal network (i.e., input, output, and ground terminals). Both the real and imaginary components of the impedance should be considered to properly represent the overall coil behavior [12]. The model of a multi-coil stator winding can be obtained from the single-coil model [13]. A three-phase induction motor can be considered as a "black-box" with one terminal for each motor phase and a terminal for the motor frame (ground). Then, the equivalence is formulated in terms of phase-to-phase and phase-to-ground impedances.

In this paper a novel equivalent circuit of the motor stator winding based on a ladder RL network is proposed. This model is valid in the range of frequency from tens of Hz to tens of kHz.

II. HF MOTOR BEHAVIOR IN THE CONDUCTED EMI FREQUENCY RANGE

The International Standards define the typical conducted EMI frequency range from 9 kHz to 30 MHz.

Impedance measurements between the terminals of different induction motors (in the low to medium power range) have shown that the resonance phenomena in the range from tens to hundreds of kHz dominate the frequency behavior of the motor winding. In particular, the presence of the coil inductance and stray capacitances leads to smoothed parallel LC resonance, and a couple of resonance peaks can be observed at frequencies around 100 kHz. For frequencies above hundreds of kHz, the winding shows a capacitive behavior. The additional resonances in the range of MHz appear as a minor phenomenon. To account for this typical behavior, the equivalent circuit shown in Fig. 1 has been adopted to represent both single-coil [12] and multi-coil AC windings [13], [14]. It can be noted that all the circuit parameters are frequency-independent. For three-phase windings, the inductive coupling among the phases is taken into account by the mutual inductances M_1 and M_2. The direct phase-to-phase capacitive coupling is neglected assuming that the corresponding capacitances are much lower than the phase-to-ground capacitances C_g.

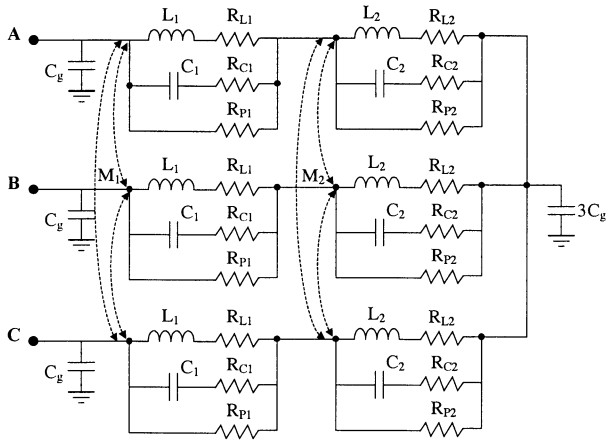

Fig. 1. HF model for a three-phase motor winding in the typical conducted EMI frequency range

In order to make the three-phase winding model fit with the experimental data, an identification problem has to be solved. The model fitting can be performed by either a trial-and-error method or numerical techniques. A procedure to get an initial estimate of the model parameters is given in [13].

To verify the proposed model for three-phase motor windings, impedance measurements were carried out at the terminals of a standard 4 kW induction motor, the data of which are given in Table I of the Appendix. The frequency behavior of both phase-to-phase and phase-to-ground impedances was investigated. A Hewlett Packard HP-4192 RLC meter was employed for the measurements, for frequency ranging from 10 kHz to 10 MHz. The measured and calculated impedance values versus frequency are shown in Figs. 2 - 5. Figs. 2 and 3 are related to the phase-to-phase impedance. Figs. 4 and 5 illustrate the behavior of the phase-to-ground impedance. The solid lines represent the numerical results obtained with the equivalent circuit, whereas the markers indicate the measured values. It can be noted a good agreement in a wide frequency range, even though the overall equivalent circuit adopt frequency-independent parameters. In this way, the proposed model can be easily employed to perform time- domain analysis of AC motor windings by standard circuit simulators.

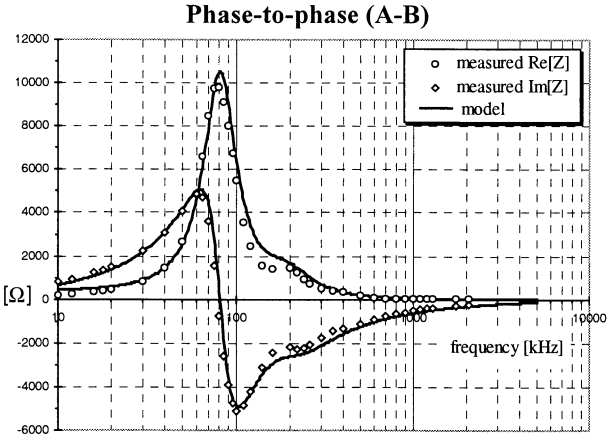

Fig. 2. Real and imaginary components of the impedance vs. frequency

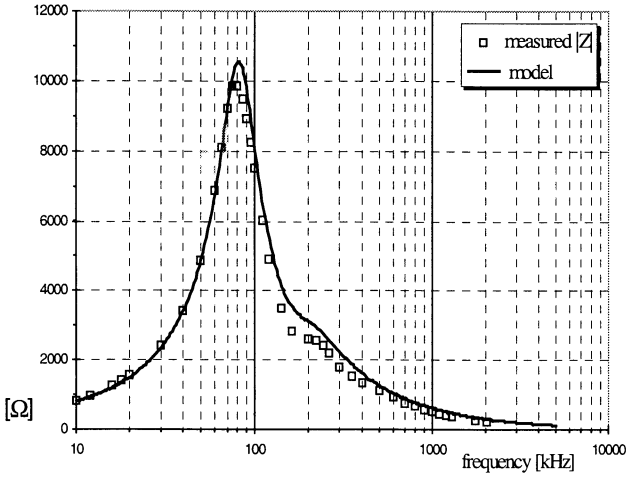

Fig. 3. Magnitude of the impedance vs. frequency

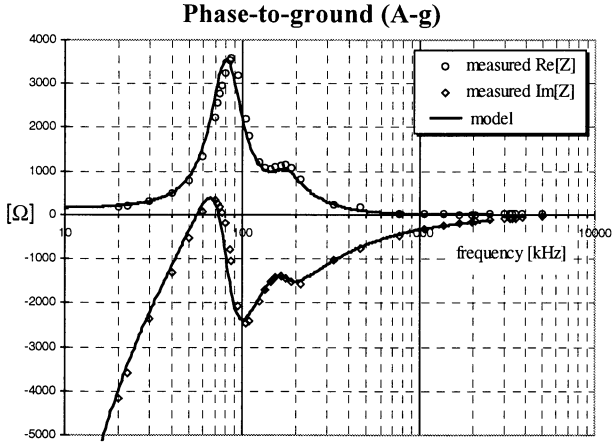

Fig. 4. Real and imaginary components of the impedance vs. frequency

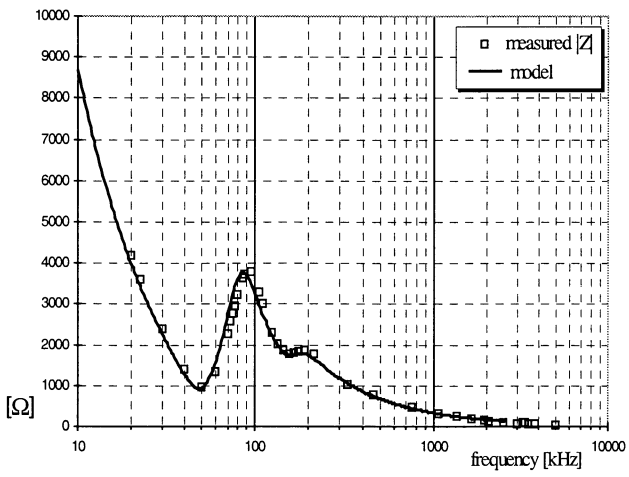

Fig. 5. Magnitude of the impedance vs. frequency

III. MOTOR BEHAVIOR BELOW THE FIRST RESONANT FREQUENCY

In order to extend the frequency range of the model below tens of kHz, the HF phenomena in both the motor stator winding and core have to be considered. In fact, impedance measurements between the phase terminals have shown that, for frequencies up to tens of kHz, the contribution of stray capacitances is not important. Skin and proximity effects in the winding and eddy currents in the laminations play a predominant role in this range of frequency. This phenomena are emphasized in Figs. 5 and 6, which show the real R_S and imaginary X_S components of the impedance measured between two phase terminals (A-B) of the induction motor under test. The procedure for obtaining the calculated values depicted in these figures is explained later.

Some works in the literature deal with these subjects. In particular, skin and proximity effects can be represented by the Dowell's approach [15], leading to analytical expressions for the winding resistance R_w and leakage inductance L_l as functions of frequency. The effects of the eddy currents in the laminations, in terms of main inductance L_m and equivalent series resistance R_c (i.e., magnetic field weakening and additional power losses in the core, respectively) can be represented on the basis of a one-dimensional electromagnetic field analysis [16]. By this approach it is possible to derive a simplified RL circuit for each phase of the stator winding, considering frequency-dependent parameters, as represented in Fig. 7. The total resistance $R(\omega)$ and inductance $L(\omega)$ are given by

$$R(\omega) = R_w + R_c, \quad \text{and} \quad L(\omega) = L_m + L_l. \tag{1}$$

For nonsaturated iron, R_c and L_m can be expressed as [16]

$$R_c(\omega) = \omega L_m^{dc} \frac{\delta_c}{s} \frac{\sinh\frac{s}{\delta_c} - \sin\frac{s}{\delta_c}}{\cosh\frac{s}{\delta_c} + \cos\frac{s}{\delta_c}}, \tag{2}$$

$$L_m(\omega) = L_m^{dc} \frac{\delta_c}{s} \frac{\sinh\frac{s}{\delta_c} + \sin\frac{s}{\delta_c}}{\cosh\frac{s}{\delta_c} + \cos\frac{s}{\delta_c}}. \tag{3}$$

In (2) and (3) $\omega = 2\pi f$, L_m^{dc} is the low-frequency inductance, s is the thickness of the lamination, and δ_c is the skin depth for the iron, $\delta_c = \sqrt{2\rho_c/\omega\mu_e}$, being ρ_c the electric resistivity of the iron sheets, and μ_e the equivalent permeability of the magnetic circuit with air gaps.

This model, with frequency-dependent parameters, has been employed in [16] to model the HF behavior of laminated iron core inductors. In this case, the winding geometry is well defined, and a single coil has to be considered. In the case of motor windings, the multi-coil configuration for each phase, the three-phase connection and the complex magnetic path for the main flux suggest to consider a different approach to derive an equivalent circuit. Furthermore, the model represented in Fig. 7 could be easily employed only for frequency-domain analysis, whereas its application to time-domain analysis could be laborious.

In order to overcome these drawbacks, the motor stator winding can be modeled by various type of RL networks, whose parameters are fitted with the results obtained by phase-to-phase and phase-to-ground impedance measurements. In particular, models consisting of series and/or parallel Foster circuits and Cauer circuits could be adopted. In this paper an equivalent circuit consisting of a ladder RL network for each phase, as shown in Fig. 8, is proposed. It has been found that four RL blocks are sufficient to model the impedance behavior in a satisfactory manner, for frequencies up to tens of kHz. The inductive coupling among the phases is neglected at this time. The model fitting, in terms of equivalent series resistance R_s and equivalent series reactance X_s, leads to the calculated values depicted in Figs. 5 and 6, respectively. A good agreement between the calculated and measured values can be observed.

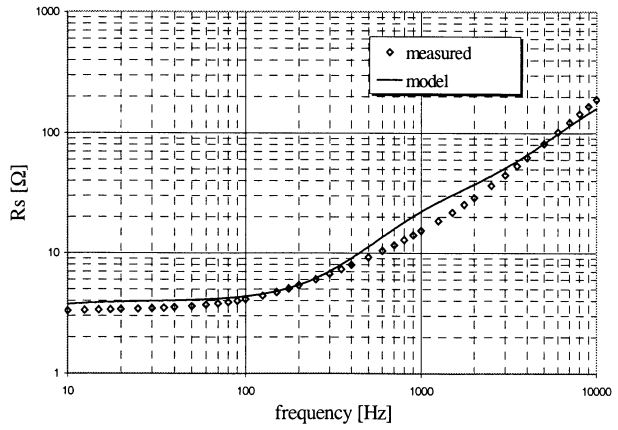

Fig. 5. Real component R_s of the impedance vs. frequency

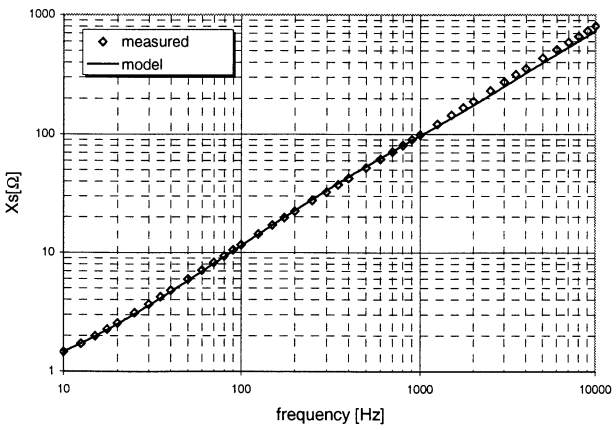

Fig. 6. Imaginary component X_s of the impedance vs. frequency

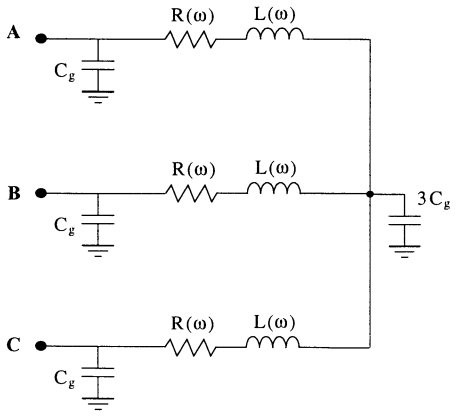

Fig. 7. Model with frequency-dependent parameters for frequencies below tens of kHz

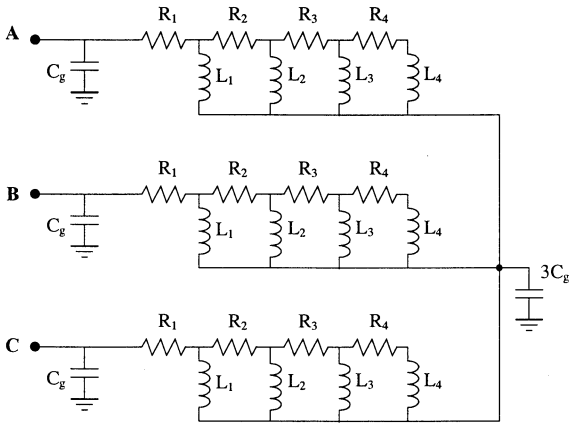

Fig. 8. Model with a ladder RL network for frequencies below tens of kHz

Furthermore, the proposed model is useful to emphasize the phase-to-phase equivalent series inductance $L_s = X_s/\omega$ seen between two motor terminals, as shown in Fig. 9. Also in this case, the agreement between calculated and measured results is good. It can be noted that the inductance halves its low-frequency value at a frequency of about 10 kHz, due to eddy currents flowing in the laminations. For higher frequencies the effects of the LC parallel resonance become important and dominate the overall frequency behavior of motor windings.

IV. CONCLUSIONS

In this paper the high-frequency behavior of induction motors with stator winding realized by mush wound coils is analyzed. A lumped equivalent circuit is proposed to represent the motor behavior in the typical conducted EMI frequency range, i.e. from tens of kHz up to tens of MHz. The model mainly accounts for the resonant phenomena occurring in this range of frequency. In particular, turn-to-turn and turn-to-ground stray capacitances strongly affect the frequency behavior of the winding. The circuit parameters are frequency-independent and are fitted with the results obtained by phase-to-phase and phase-to-ground impedance measurements. In this way, the proposed model can be easily implemented on standard circuit simulators to analyze and predict the HF behavior of the stator winding when the motor is supplied by switching converters. In particular, conducted common- and differential-mode interferences can be investigated.

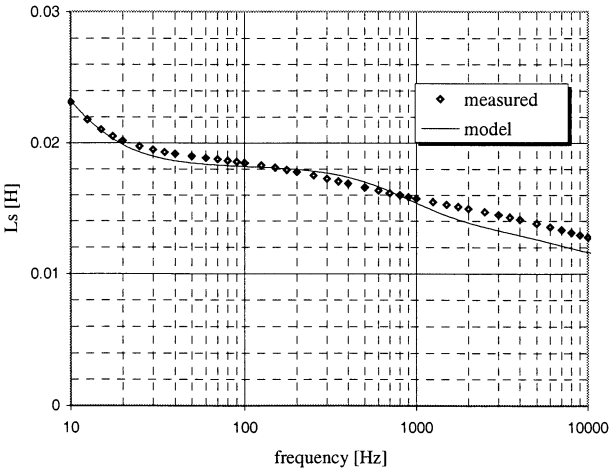

Fig. 9. Equivalent series inductance L_s vs. frequency

In order to extend the frequency range of the model below tens of kHz, an equivalent circuit of the motor stator winding consisting of a ladder RL network for each phase is proposed. The model accounts for skin and proximity effects in the stator winding and eddy currents in the iron core. Also in this case, the model fitting can be performed on the basis of phase-to-phase and phase-to-ground impedance measurements. By means of this circuit it is possible to represent the frequency behavior of the motor stator winding up to tens of kHz, which are the typical values for the switching frequency of the supply inverter.

V. APPENDIX

TABLE I
Three-phase induction motor data

Power	Voltage, Frequency	Speed	Cooling
4 kW	220/380 V, 50 Hz	2800 rpm	coaxial fun

VI. REFERENCES

[1] L. Gubbala, A. von Jouanne, P. Enjeti, C. Singh, H. Toliyat, "Voltage Distribution in the Windings of an AC Motor Subjected to High dv/dt PWM Voltages," *Proc. of PESC Conf.*, June 1995, Atlanta (USA), pp. 579-585.

[2] Z. Krzemien, "The Additional Phenomena which Appear in Induction Motors Fed from PWM Inverters," *European Conf. on Power Electronics & Applications, EPE*, September 1997 - Trondheim (N), pp. 2.515-2.519.

[3] D. Maly, D.W. Novotny, C. Thompson, "The Influence of Winding Capacitance on High Frequency Time Harmonic Losses in Induction Motors," 0-7803-0634-1/92, *IEEE*, pp. 33-39.

[4] Y. Murai, T. Kubota, Y. Kawase, "Leakage Current Reduction for a High-Frequency Carrier Inverter Feeding an Induction Motor," *IEEE Trans. on Ind. Appl.*, Vol. 28, No. 4, July/Aug 1992, pp. 858-863.

[5] E. Zhong, S. Chen, T.A. Lipo, "Improvements in EMI Performance of Inverter-Fed Motor Drives," *Proc. of APEC*, March 1994, pp. 608-614.

[6] E. Zhong, T.A. Lipo, J.R. Jaeschke, D. Gritter, "Analytical Estimation and Reduction of Conducted EMI Emission in High Power PWM Inverter Drives," *Proc. of PESC Conference*, June 1996, Baveno (IT), pp. 1169-1175.

[7] L. Ran, S. Gokani, J. Clare, K.J. Bradley, C. Christopoulos, "Conducted electromagnetic emissions in induction motor drive systems. Part I: Time domain analysis and identification of dominant modes, Part II: Frequency domain models," *IEEE Trans. on Power Electronics*, Vol. 13, No. 4 , July 1998, pp. 757 –776.

[8] L. Tihanyi, *Electromagnetic compatibility in power electronics*. IEEE Press 1995, New York (USA).

[9] G. Grandi, I. Montanari, U. Reggiani, "Effects of power converter parasitic components on conducted EMI," *International Zurich Symposium on EMC*, February 18-20, 1996, Zurich (CH), pp. 499-504.

[10] M.T. Wright, S.J. Yang, K. McLeay, "General Theory of Fast-Fronted Interturn Voltage Distribution in Electrical Machine Windings," *IEE Proc. Part. B*, Vol. 130, No. 4, July 1983, pp. 245-256.

[11] R.G. Rhudy, E.L. Owen, D.K. Sharma, "Voltage Distribution Among the Coils and Turns of a Form Wound AC Rotating Machine Exposed to Impulse Voltage," *IEEE Trans.*, Vol. EC-1, No. 2, June 1986, pp. 50-60.

[12] G. Grandi, D. Casadei, U. Reggiani, "Equivalent Circuit of Mush Wound AC Windings for High Frequency Analysis," *Proc. ISIE Conf.*, July 1997, Guimarães (PT), pp. SS.201-SS.206.

[13] G. Grandi, D. Casadei, A. Massarini, "High Frequency Lumped Parameter Model for AC Motor Windings," *European Conf. on Power Electronics & Applications, EPE*, Sept. 1997 - Trondheim (N), pp. 2.578-2.583.

[14] G. Suresh, H.A. Toliyat, D.A. Rendusara, P.N. Enjeti, "Predicting the transient effects of PWM voltage waveform on the stator windings of random wound induction motors," *IEEE Trans. on Power Electronics*, Vol. 14, No. 1, Jan. 1999, pp. 23-30.

[15] P.J. Dowell, "Effects of eddy currents in transformer windings," *Proc. Inst. Elect. Eng.*, vol. 113, pp. 1387-1394, Aug. 1966.

[16] U. Reggiani, G. Grandi, G. Sancineto, M.K. Kazimierczuk, and A. Massarini, "High-frequency behavior of laminated iron-core inductors for filtering applications," in *Proc. IEEE APEC*, 2000, pp. 654-660.